Available online at www.sciencedirect.com
ScienceDirect
Biochimica et Biophysica Acta 1768 (2007) 628–636
Biochimica et Biophysica Acta
BBA
www.elsevier.com/locate/bbamem

Shiga toxin B-subunit sequential binding to its natural receptor in lipid membranes

David G. Pina [a,*,1], Ludger Johannes [b], Miguel A.R.B. Castanho [a]

[a] *Centro de Química e Bioquímica, Faculdade de Ciências da Universidade de Lisboa, Campo Grande C8, 1749-016 Lisboa, Portugal*
[b] *Laboratoire Trafic et Signalisation, UMR 144 CNRS, Institut Curie, 26 rue d'Ulm, 75248 Paris Cedex 05, France*

Received 18 August 2006; received in revised form 13 November 2006; accepted 5 December 2006
Available online 23 December 2006

Abstract

Shiga toxin B-subunit (STxB), a protein involved in the cell-binding and intracellular trafficking of Shiga holotoxin, binds to a specific glycolipid, the globotriaosyl ceramide (Gb_3). Tryptophan residues of STxB, located at the protein–membrane interface, allow one to study its interaction with model membranes by means of spectroscopic methods with no need for chemical derivatisation with a fluorophore. The protein emits maximally around 346 nm and a blue shift of about 8 nm, as well as the occurrence of changes in the emission fluorescence intensity spectra, is indicative of insertion and partition into the membrane. However, the interaction seems to take place without pentamer dissociation. Acrylamide quenching experiments confirm tryptophan residues become less exposed to solvent when in the presence of vesicles, and the use of lipophilic probes suggests that they are located in a shallow position near the water/membrane interface. Fluorescence intensity and lifetime measurements upon STxB titration with Gb_3-containing vesicles suggest a complex STxB/Gb_3 docking mechanism involving static quenching in the later stages. Based on our observations, a model of the protein–membrane interaction is proposed and the STxB membrane partition and binding constants were calculated.

Keywords: Shiga toxin B-subunit; Globotriaosyl ceramide; Fluorescence; Lipid vesicles

1. Introduction

Shiga toxin is a bacterial protein produced by *Shigella dysenteriae* and is structurally related to verotoxins and cholera toxin, all of which belong to the AB_5 toxins family [1]. It is composed of two subunits with distinct functions. Infections with bacteria producing Shiga and Shiga-like toxins are responsible for widespread disease and for the death of a large number of humans [2], and increasing knowledge about the toxin–cell interaction is a fundamental requisite for the efficient production and application of molecules that might help to treat those types of infections. The monomeric A-subunit has a *N*-glycosidase enzymatic activity leading to the inhibition of protein synthesis and cell death, whereas the B-subunit (STxB) is a homopentamer responsible for the receptor binding, internalisation and intracellular transport of the holotoxin [3–6]. STxB has been extensively used in cell biology research as a tool for the characterisation of the so-called retrograde transport, a pathway going directly from early endosomes to Golgi apparatus and ER in some cell types [7–11].

The Shiga toxin receptor is a glycosphingolipid termed globotriaosyl ceramide (Gb_3 or CD77), being STxB among the smallest known lectins [12]. It is strongly expressed on human tumors [13,14] and the use of STxB in cancer therapy has been suggested [15–18]. STxB is also developed as a vector to bring epitopes into the cytosol [19], as it has been shown that B-subunit alone is fully functional in terms of membrane binding

Abbreviations: STxB, Shiga toxin B-subunit; CD, circular dichroism; LUV, large unilamellar vesicles; Trp, tryptophan; Gal, galactose; Glc, glucose; Suc, sucrose; POPC, 1-palmitoyl-2-oleyl-*sn*-glycero-3-phosphocholine; DPPC, 1,2-dipalmitoyl-*sn*-glycero-3-phosphocholine; POPG, 1-palmitoyl-2-oleyl-*sn*-glycero-3-[phospho-rac-(1-glycerol)]; 5NS, 5-doxyl-stearic acid; 16NS, 16-doxyl-stearic acid

* Corresponding author. Tel.: +44 1223 767042; fax: +44 1223 336362.
E-mail address: dgp28@cam.ac.uk (D.G. Pina).
[1] Present address: Department of Chemistry, University of Cambridge, Lensfield Road, Cambridge CB2 1EW, UK.

0005-2736/$ - see front matter © 2007 Elsevier B.V. All rights reserved.
doi:10.1016/j.bbamem.2006.12.011

and intracellular trafficking [20,21]. While the A-subunit of Shiga toxin apparently uses the retrotranslocation machinery to have access to the cytosol [22], as do other protein toxins [23], it is not clear by what mechanism STxB crosses membranes in antigen presenting cells even though such translocation has clearly been shown [24]. Neither is it known if the interaction of STxB with the membranes induces conformational changes on the protein. The aim of this study is to understand the interaction of STxB with model membranes.

STxB is composed of five identical monomers of 69 residues (7.7 kDa). The three-dimensional structure of STxB and holotoxin has been solved both by NMR and X-ray crystallography, showing for the B-subunit a pentameric ring-like conformation with a central pore delimited by α-helices from each monomer and surrounded by antiparallel β-sheets [25–27]. Each monomer is thought to have up to three binding sites for Gb_3 molecules (reported as site 1, 2, and 3) [28], although NMR studies suggest only one molecule is bound per monomer [29]. This could be the situation existing in physiological conditions, as it seems not all three binding sites are relevant for binding. The first binding site is located at the cleft of adjacent monomers and involves hydrophobic stacking interaction of Phe30 residue with the terminal Gal of receptor and hydrogen bonds with proximal polar residues. Site 2, believed to be the higher affinity binding site, is located in the opposite side of Phe30 phenyl ring and involves mainly hydrogen bonds with the trisaccharide. Finally, it is believed Trp34, just at the beginning of each one of the α-helix motifs, interacts with Gb_3 by hydrophobic stacking in the third binding site. However, receptor binding can still occur after deleting the Trp residue [30]. Trp residues are located in the protein membrane interface and are solvent exposed in the native 3D-crystal conformation (Fig. 1).

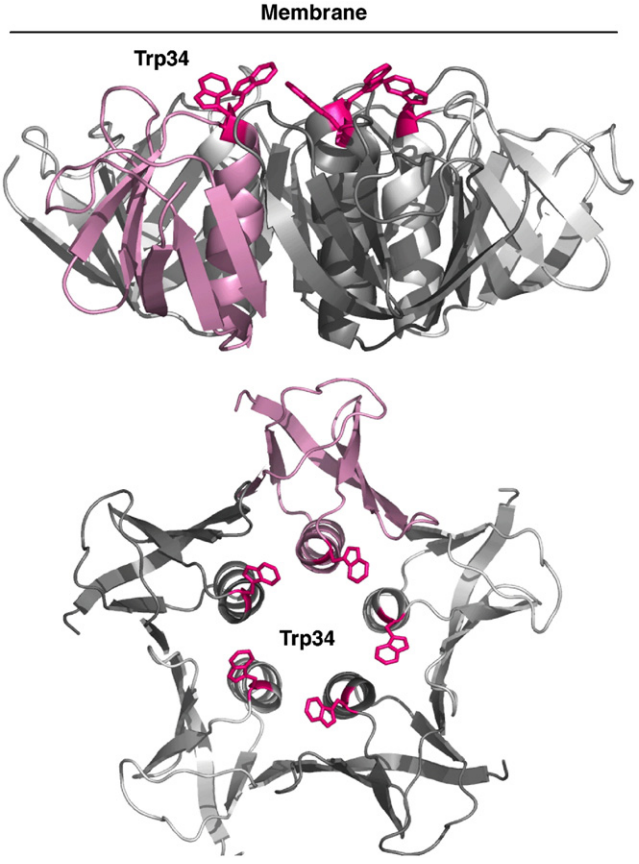

Fig. 1. Localisation of tryptophan residues in the STxB three-dimensional structure. Trp residues are solvent exposed in aqueous buffer and located at the protein–membrane interface when in presence of vesicles. Figure was produced with the PyMol software program using X-ray crystallographic coordinates from Brookhaven PDB ID 1BOS.

The position of Trp within STxB structure enables the application of fluorescence spectroscopy techniques for the study of its interaction with lipid vesicles with no need of derivatisation with a fluorescent probe. A previous paper reports fluorescence spectroscopy studies on the STxB interaction with Gb_3-containing vesicles before the protein's three-dimensional structure was determined [31]. The main observations were the existence of a solvent-exposed Trp in solution (later confirmed by the 3D-structure determination) and the occurrence of a blue shift and increase in fluorescence emission intensity upon addition of Gb_3-containing membranes. However, these studies were performed in small unillamelar vesicles (SUV), which have an artefact-generating high curvature radius. Moreover, no physical explanation of the process observed was stated. In this paper we have characterised the photophysics of STxB in aqueous buffer and in presence of large unillamelar vesicles (LUV) of different lipid composition and Gb_3, mainly by means of steady-state and time-resolved fluorescence spectroscopy, to obtain insights about the mode of interaction of the protein with lipid membranes and propose a physical model.

2. Materials and methods

2.1. Materials

POPC (1-palmitoyl-2-oleyl-*sn*-glycero-3-phosphocholine), POPG (1-palmitoyl-2-oleyl-*sn*-glycero-3-[phosphor-rac-(1-glycerol)]) and DPPC (1,2-dipalmitoyl-*sn*-glycero-3-phophocholine) were purchased from Avanti Polar-Lipids (Alabaster, AL), and globotriaosylceramide (Gb_3) from Matreya LLC (Pleasant Gap, PA). Cholesterol was from Sigma (St. Louis, MO) and 5NS (5-doxyl-stearic acid) and 16NS (16-doxyl-stearic acid) were from Aldrich Chem. Co. (Milwaukee, WT). HEPES, NaCl, L-tryptophan, acrylamide, ethanol, chloroform, D-Galactose, D-Glucose, D-Sucrose and urea were purchased from Merck (Darmstadt, Germany).

2.2. Protein preparation

Recombinant B-subunit was expressed in *E. coli* by heat induction at 42 °C of a pSU108 plasmid containing the STxB gene sequence, and was purified by an osmotic shock procedure followed by two consecutive chromatography steps, first an anion exchange column followed by an affinity column, as described elsewhere [32]. Purity of the samples were checked by Tris/Tricine SDS-PAGE, and protein concentration was determined spectroscopically using the extinction coefficient value of 9500 M^{-1} cm^{-1} at 278 nm for the monomer [33]. 10 mM HEPES, pH 7.4, 150 mM NaCl buffer was used throughout all studies (aqueous buffer) and experiments were carried out at 20 °C.

2.3. Vesicles preparation

Large unilamellar vesicles (LUV), with typical 100 nm diameter were prepared by the extrusion method described elsewhere [34]. All glycolipid-containing LUV were prepared with 5 mol% Gb_3. Lower contents of Gb_3 was

not inducing the observed increase in fluorescence intensity, probably due to experimental limitations.

2.4. CD spectroscopy

CD spectra in the far-UV (200–250 nm) were recorded in a Jasco J720 spectropolarimeter, using a 1 mm path length circular cuvette. The protein concentration was ca. 0.02 mM. Spectra are averages of five scans and were all background-corrected, smoothed using J720 noise reduction software and converted to molar ellipticity ($[\Theta]=M_{res}\,\Theta_{obs}\,l^{-1}\,p^{-1}$), where $M_{res}=111.5$ is the mean residue molar mass (in daltons), Θ_{obs} is the ellipticity measured (degrees) at wavelength λ, l is the optical path length of the cell (mm) and p is the protein concentration (mg/ml).

2.5. Steady-state fluorescence studies

STxB has a tryptophan residue per monomer, which make fluorescence techniques suitable tools. All fluorescence measurements were performed with a Fluorolog-3 spectrofluorimeter from Jobin-Yvon/Horiba, and acquired with DataMax v2.20 software programme. Samples were excited at 280 nm (for REES experiments excitation wavelength varied from 280 to 300 nm) and emission spectra were collected from 300 to 450 nm and were blank corrected. All spectra were also corrected with the instrumental correction function. Excitation and emission slits with a 4 nm bandpass were used for all measurements.

Membrane partition studies were performed by successive additions of small volumes of LUV (stock concentration of 15 mM) to a 0.4 ml sample with ca. 0.01 mM protein, with a 10 min incubation in between. Fluorescence intensity data were corrected for dilution and inner filter effects.

Fluorescence anisotropy was calculated from:

$$r=\frac{I_{vv}-GI_{vh}}{I_{vv}+2GI_{vh}} \tag{1}$$

The two subscripts in I are used to indicate the orientation of the excitation and emission Glan–Thompson polarizers, respectively (v—vertical, h—horizontal). $G=I_{hv}/I_{hh}$ is an instrumental correction factor.

2.6. Time-resolved fluorescence studies

Fluorescence lifetimes acquisitions were monitored using the TCSPC accessory, with a 280 nm LED laser source (IBH, UK). Lifetimes were calculated from time-resolved fluorescence intensity decays using 10 Kcounts in the peak channel. Fluorescence intensity decay curves were deconvoluted with the instrument software DAS6 (IBH, UK) and analysed as a sum of exponential terms. The mean average lifetime, $\langle\tau\rangle$ is:

$$\langle\tau\rangle=\frac{\sum a_i\tau_i^2}{\sum a_i\tau_i} \tag{2}$$

a_i is the pre-exponential factor and τ_i is the fluorescence lifetime of each i component [35]. The goodness of the fit was judged from the global chi-square value and weighted residuals.

2.7. Quenching experiments

Quenching studies were carried out by successive additions of small amounts of acrylamide, galactose, glucose and sucrose stocks. Excitation wavelength was 280 nm, except for acrylamide titration where it was set at 290 nm to minimise the relative quencher/fluorophore light absorption ratio, and inner filter effect was negligible under these experimental conditions.

Data were fitted by the Stern–Volmer equation [35]:

$$\frac{I_0}{I}=1+K_{SV}[Q] \tag{3}$$

where I_0 and I are the fluorescence intensities in the absence and presence of the quencher (acrylamide or carbohydrates), respectively, $[Q]$ is the molar quencher concentration, and K_{SV} is the Stern–Volmer constant.

Membrane in-depth location of STxB Trp residues was studied using 5NS or 16NS as quenchers [36]. Titration of ca. 0.01 mM STxB in presence of 1.5 mM POPC/Gb_3 LUV was carried out by addition of aliquots of 5NS and 16NS stock solutions (70 mM in ethanol). Final ethanol concentration was kept below 2% (v/v). Assays were followed at $\lambda_{ex}=290$ nm and $\lambda_{em}=340$ nm.

3. Results and discussion

3.1. Photophysical characterisation of STxB

The spectral characteristics of STxB are dominated by the 5 Trp residues (one in each monomer). Interaction of the protein with LUV can be followed by the changes in several spectroscopic parameters, namely, fluorescence intensity, spectral shifts, and fluorescence lifetimes. Normalised emission fluorescence spectra of STxB in aqueous buffer and in the presence of 1.5 mM of POPC/Gb_3 vesicles are represented in Fig. 2A. In aqueous buffer, the emission intensity maximum wavelength (λ_{max}) occurs at ~346 nm (after blank and instrumental correction), indicating solvent exposure of Trp residues (free Trp emits maximally at ~350 nm under the same experimental conditions). Upon addition of LUV, λ_{max} is blue shifted to a maximum of ~338 nm. This is an evidence of the interaction of the protein with the model membranes. However, the far-UV CD spectrum of STxB in the presence of vesicles is

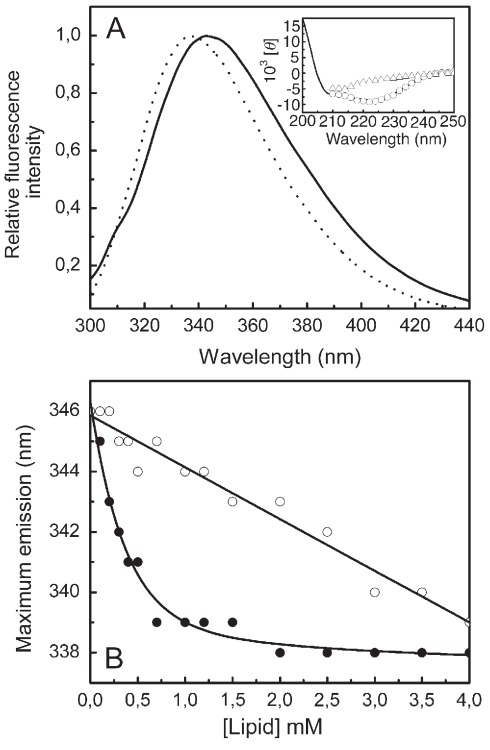

Fig. 2. Photophysical characterization. (A) Normalised emission spectra ($\lambda_{exe}=280$ nm) for STxB in aqueous buffer (solid line) and in the presence of 1.5 mM POPC/Gb_3 (dotted line) LUV. Inset shows changes of molar ellipticity in the far-UV CD region for STxB in aqueous buffer (solid line), 1.5 mM POPC/Gb_3 vesicles (○), and 8 M urea (△). (B) Changes in maximum intensity emission wavelength as a function of POPC/Gb_3 (●) and pure POPC (○) concentration.

not significantly perturbed compared to the native protein in solution (inset in Fig. 2A). Thus, it seems that addition of LUV do not induce major conformational changes in the protein secondary structure, and STxB retains its pentameric conformation when interacting with membranes (the spectrum of STxB dissociation in the presence of 8 M urea is shown). Although separation of the pentamer into five monomers retaining their secondary-level structure upon interaction with lipids could, in principle, be speculated, steady-state anisotropy data do not support this hypothesis. Immobilisation of monomers in the membrane matrix would lead to an increased value of fluorescence anisotropy. At variance, the measured fluorescence anisotropy remains constant ($r \sim 0.03$–0.06). Such a low value in a viscous medium and moderate excited-state lifetime species like Trp residues in lipid bilayers can only be due to energy migration depolarisation [37]. Significant energy migration occurs when fluorophores are in close vicinity of each other, which is the case for tryptophan residues in the STxB pentamer, as the distance between each indole group is 4–6 Ånsgtrom (see Fig. 1), according to the available crystallographic data [25,26].

The same qualitative blue shift and vibrational progression (i.e. the "shape" of the spectra) described before were obtained when incubating STxB with vesicles composed of other lipids. STxB is slightly acidic (pI = 5.7) and has a negative charge at neutral pH. However, the pH at the proximity of the membrane surface is believed to be lower, and STxB probably has a negligible charge in this microenvironment. Thus, no significant effect on the STxB interaction with membranes was observed when negatively charged POPC:POPG (80:20), gel phase forming lipid, DPPC, and cholesterol-containing, i.e. POPC:Cholesterol (82:18 and 67:33) vesicles were tested (cholesterol decreases membrane fluidity at room temperature). Nevertheless, the blue shift observed in the presence of Gb_3-free vesicles is linearly LUV concentration-dependent, whereas it is exponentially dependent for Gb_3-containing vesicles (Fig. 2B). This is probably due to the more efficient incorporation of protein in the presence of its natural receptor, reaching saturation at ~1.5 mM lipid concentration, whereas the spectral changes observed with Gb_3-free vesicles are non-specific. These results do not agree with a previous report stating that no interaction occurs between STxB and Gb_3-free vesicles [31].

3.2. Red edge excitation shift

The red edge excitation shift (REES), usually observed for mobility restricted polar fluorophores, can be described as the increase in the wavelength of maximum emission observed when the excitation wavelength is gradually shifted towards the red edge of the absorption band. Thus, REES is appropriate to obtain information on the organisation and dynamics of the fluorophore environment, including Trp residues in proteins [38,39]. The variation of the wavelength of maximum emission with the increase of the excitation wavelength for STxB in aqueous buffer, and in the presence of vesicles is presented in Fig. 3. A large REES (~17 nm when excitation wavelength varies from 280 to 300 nm) is observed for native STxB in aqueous buffer. This observation is very uncommon, as REES is usually observed only in viscous or in mobility restricted conditions and in proteins with maximum emission wavelengths between 325 and 340 nm (when $\lambda_{ex} = 280$ nm) [38]. In our case, although STxB pentamers do not aggregate in solution (as confirmed by analytical ultracentrifugation experiments [40]), the particular organisation of Trp residues in the pentamer conformation (see Fig. 1) can imply a restriction in mobility and affect their photophysical properties. Supporting this hypothesis is the observation that when STxB is chemically unfolded and dissociated by incubation with 8 M urea, although being a more viscous solution, a REES of only 4 nm is observed when the excitation wavelength is changed from 280 to 300 nm (open circles in Fig. 3) confirming the increase of Trp mobility compared with the native conformation. Denatured proteins exhibiting REES are scarce because this observation means that Trp residues are partially shielded from the bulk solvent [41]. The presence of lipid does not significantly change REES in comparison to the aqueous buffer conditions as STxB maintains its pentameric structure when in contact with membranes (see above).

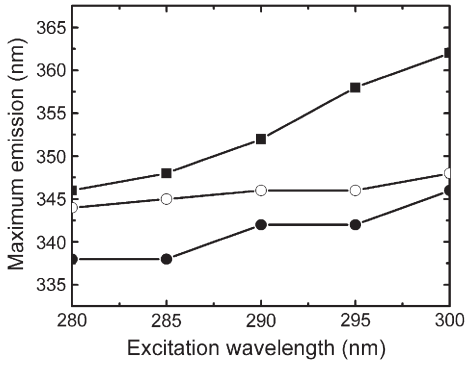

Fig. 3. Red-edge excitation shift. Variation of maximum intensity wavelength of the emission spectra at different excitation wavelengths for STxB in aqueous buffer (■), in presence of 1.5 mM POPC/Gb_3 vesicles (●), and denatured by 8 M urea (○). Each point is the average of two determinations and lines are merely guides to the eye.

3.3. Fluorescence quenching

In order to evaluate the localisation of Trp residues of STxB when interacting with the model membranes, fluorescence quenching by the lipophilic probes 5NS and 16NS was used. These two derivatised fatty acids differ in the position of the quencher moiety (doxyl) along the hydrocarbon chain. Thus, they are used to determine the depth of the fluorophore in the membrane, by comparing the quenching results obtained with each of them. Steady-state fluorescence quenching measurements were performed with fixed concentrations of STxB and lipid, and increasing concentration of quenchers. Fig. 4A shows the variation of I_0/I as a function of local lipophilic probe concentration in membranes for STxB in the presence of 1.5 mM POPC/Gb_3 vesicles. It is clear that STxB Trp fluorescence is more extensively quenched by the 5NS probe

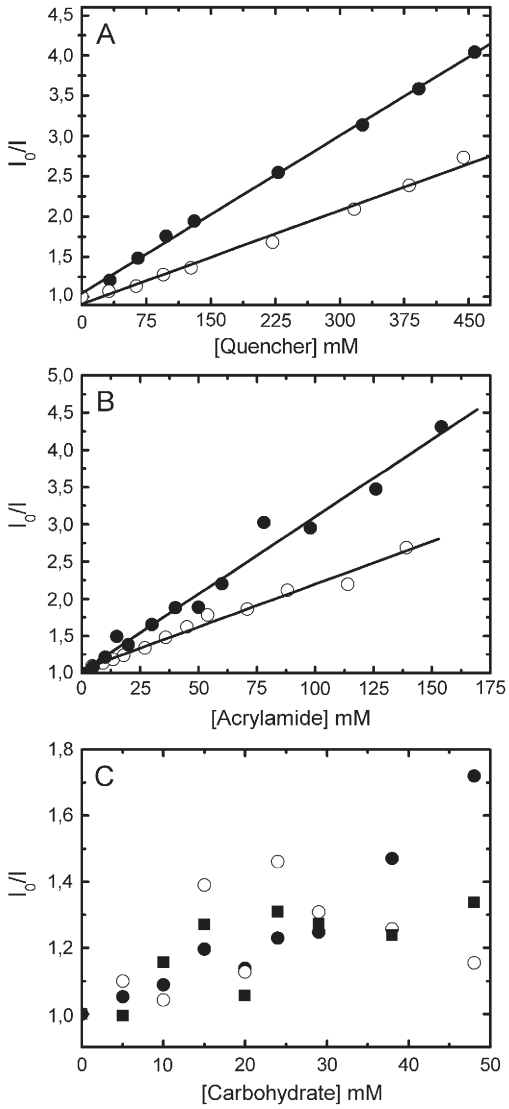

Fig. 4. Stern–Volmer plots. (A) Quenching by the derivatised lipophilic molecules 5NS (●) and 16NS (○) in the presence of 1.5 mM POPC/Gb_3 vesicles. (B) Quenching by acrylamide of STxB in buffer (●), and in presence of 1.5 mM POPC/Gb_3 vesicles (○). (C) Quenching by different carbohydrates: galactose (●), glucose (○), and sucrose (■).

(K_{SV}=6.54±0.09 M^{-1}) as compared to 16NS (K_{SV}=3.88±0.15 M^{-1}), suggesting that the fluorophore is located in a shallow position at the water/membrane interface. This confirms that the protein's structural motifs are not being significantly perturbed by the presence of membranes.

The effect of acrylamide on the STxB Trp fluorescence is represented in Fig. 4B. Linear Stern–Volmer plots are indicative of all Trp residues being fairly accessible to acrylamide. STxB in aqueous buffer has a K_{SV}=20.8±0.9 M^{-1}, similar to that reported for the model compound N-acetyltryptophanamide, NATA [42], and upon addition of LUV K_{SV} decreases twofold (K_{SV}=11.5±0.5 M^{-1}), due to the involvement of Trp residues in the protein–membrane interaction. Previous work stated a non-linear Stern–Volmer plot for the protein in the absence of lipid that we were not able to detect [31,43]. According to our data static and dynamic quenching do not co-exist.

Titration of STxB with different carbohydrates shows a quenching of STxB Trp in the presence of galactose, glucose and sucrose saccharides up to 40–50 mM concentration (Fig. 4C), with no alteration of lifetimes values (data not shown). Taking into account the local glycolipid concentration in the membrane volume itself (ca. 65 mM when considering the lipid molar volume to be 0.763 dm^3 mol^{-1} [44]), the Gb_3 carbohydrate moiety can have a noticeable quenching effect on the STxB fluorescence.

3.4. Determination of partition and binding constants

Fluorescence intensity of STxB titrated with 5 mol% Gb_3-containing POPC vesicles increases until reaching a maximum at 1.5 mM lipid concentration, followed by a decrease (solid circles in Fig. 5). This is a unique characteristic of Gb_3-containing vesicles, since the absence of it induces a slight decrease of fluorescence intensity for all lipid composition vesicles tested (open circles in Fig. 5). This observation is in contrast with a regular increase of average fluorescence lifetime, $\langle\tau\rangle$, for POPC/Gb_3 LUV titration (solid squares in Fig. 5). $\langle\tau\rangle$ for STxB is described by a sum of not less than three exponentials, with a mean lifetime of 4.3 ns in aqueous solution. In the presence of POPC/Gb_3 vesicles, this value is increased (up to 7.3 ns for [L]= 3.0 mM). Lifetimes constantly increase upon Gb_3-containing vesicles addition, even after reaching the maximum fluorescence intensity at ~1.5 mM lipid concentration. $\langle\tau\rangle$ for other LUV compositions were determined (DPPC, POPC:POPG), with no significant changes compared to STxB in aqueous buffer. Even the insertion of 10 mol% of a monossacharide-acyl in liposomes had the same effect as pure vesicles, confirming the specificity of spectral changes observed only for the interaction between the Gb_3 trisaccharide moiety and STxB. Therefore, partition into Gb_3-free vesicles causes quenching of STxB fluorescence, which is mainly static, while Gb_3-containing vesicles cause an increase on fluorescence intensity first (up to 1.5 mM lipid concentration) and a pronounced static quenching afterwards.

In a first attempt to quantify the extent of interaction of STxB with the membrane, the apparent partition coefficient between

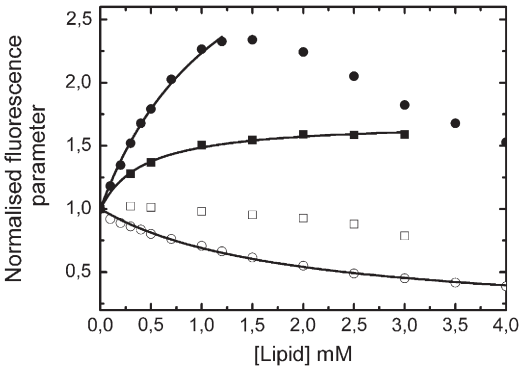

Fig. 5. Membrane partition curves. Titration curves of STxB as a function of POPC/Gb_3 (●, ■) and pure POPC (○, □) concentration obtained from fluorescence intensity (●, ○) and lifetimes (■, □) experiments. Lines represent non-linear regression fits (see text for details).

the lipid and aqueous phases, $K_{p,App}$, was determined using a derived formalism based on the fluorescence lifetime averaged by the pre-exponentials, $\overline{\tau}$:

$$\overline{\tau} = \frac{\sum a_i \tau_i}{\sum a_i} \quad (4)$$

The use of $\overline{\tau}$ instead of $\langle\tau\rangle$ for the $K_{p,App}$ calculation is advantageous because it does not require the knowledge of the molar absorptivity, and consequent errors related to its determination are avoided. $K_{p,App}$ can be obtained from the following relationship (see appendix of [45] for details):

$$\frac{\overline{\tau}}{\overline{\tau}_W} = \frac{1 + \frac{\overline{\tau}_L}{\overline{\tau}_W} K_p \gamma_L [L]}{1 + K_p \gamma_L [L]} \quad (5)$$

where $\overline{\tau}_W$ and $\overline{\tau}_L$ are the fluorescence lifetimes averaged by the pre-exponentials for STxB in the aqueous and membrane phase, respectively, γ_L is the molar volume of the phospholipids, which for POPC corresponds to 0.763 M^{-1} [42], and [L] is the molar lipid concentration accessible to the protein (the outer leaflet of the bilayer, i.e. half of the total lipid concentration). By the non-linear regression fit of $\overline{\tau}/\overline{\tau}_W$ versus [L] data (line through solid squares in Fig. 5), one obtains an apparent $K_{p,App}$ of $(6.2\pm0.5)\times10^3$, which corresponds to a ΔG of -7.4 kcal mol^{-1}. A more detailed and realistic description of the STxB/Gb_3 interaction is to consider the combined effect of STxB partition to membranes, subsequent Gb_3 docking to a specific binding site (an increase in quantum yield resulting there from) and, finally, docking to the remaining binding sites, leading to the static quenching observed at higher lipid concentrations. Fig. 6 illustrates this model. However, while this model appears the most plausible to us, other interpretations cannot be excluded. If one considers the interaction between STxB and non-Gb_3 containing vesicles only, i.e. the interaction between the protein and the membrane surface before Gb_3 contacts with the binding sites, K_p can be calculated from changes in intensity upon lipid addition (open circles in Fig. 5) using the analogue formalism I/I_w (see equation in [46]). K_p for pure POPC vesicles is $(1.4\pm0.2)\times10^3$.

The binding constant (K_B in Fig. 6) can be calculated using a more complex formalism (derived in Appendix), which accounts for simultaneous partition and binding. For the sake of simplicity it was assumed that docking to the last binding sites only occurs when the first binding site is completely saturated. The biphasic dependence observed in Fig. 5 (solid circles) supports this to a reasonable approximation. Non-linear regression analysis on the data up to 1.2 mM lipid concentration leads to a K_B of 0.0123 ± 0.0051 mM^{-1}. Whilst at a first glance this value may seem well below others that have been reported in the literature [47], it should be stressed that this K_B refers to the local concentration in the membrane, whereas an apparent constant referring to bulk analytical concentrations would be much higher (by three orders of magnitude, depending on [L]) but a poorer description of the process at the molecular level (see Appendix for further details). It is the combined effect of membrane partition and binding in the confined space of the membrane that favors STxB/Gb_3 association.

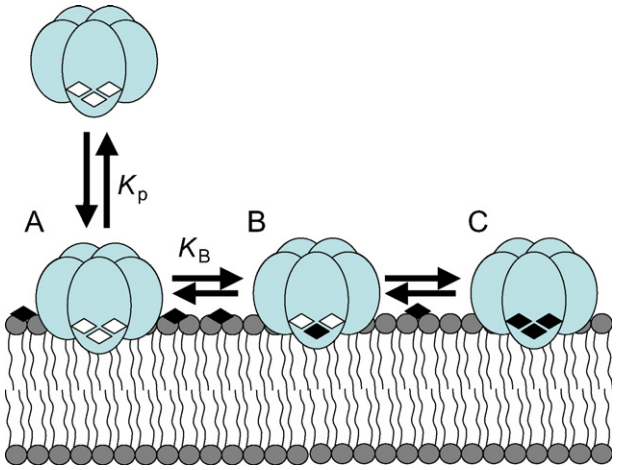

Fig. 6. Schematic representation of the proposed interaction between STxB and Gb_3-containing lipid vesicles. STxB is a soluble globular pentamer in solution and binds to its natural receptor, the glycolipid Gb_3 (solid diamonds-glycidic moieties) in membranes after an intermediate step of direct interaction with lipids (A). Once at the membrane surface with empty binding sites, STxB remains pentameric in a shallow position and suffers small structural changes leading to a slight static quenching of Trp fluorescence. It probably has the ability to cluster Gb_3 molecules in its vicinity, as 5 to 15 binding sites (empty diamonds) have been reported per pentamer. When few Gb_3 molecules are available for binding, nearly all dock in high affinity binding sites (B), which do not directly involve Trp residues. However, docking to these sites induce changes in their Trp excited-state lifetimes and fluorescence quantum yields probably via local conformational changes. Once high-affinity binding sites are saturated, all binding sites are occupied by Gb_3 molecules, including the ones in direct contact with Trp, which lead to a static quenching of fluorescence intensity (C).

4. Conclusion

STxB interacts with model membranes, independent of its lipid composition, as supported by changes in fluorescence intensity and blue shifts occurring upon addition of LUV, without significant secondary structure conformational changes (as indicated by CD experiments). However, in pure POPC vesicles, the protein seems to interact non-specifically with the membrane surface leading to a slight decrease in fluorescence intensity and excited-state lifetimes. The presence of 5 mol% of Gb_3 glycolipid receptor induces an increase in fluorescence intensity as well as lifetimes. Several studies have shown that Shiga toxin is associated with detergent resistant membranes [9,48,49] suggesting microdomains clustering in biological membranes. If Gb_3 was associated with nanoclusters, as recently suggested for GPI-anchored proteins [50], this could favor the initial binding to membranes. As a consequence, the relatively high glycolipid concentration *in vitro* can be interpreted as the accumulation of Gb_3 in lipid rafts *in vivo*. Fluorescence intensity reaches a maximum at 1.5 mM of POPC/Gb_3 vesicles, followed by a progressive decrease, which is not accompanied by lifetimes. Lifetimes reach a plateau. A REES value of ~17 nm for STxB in aqueous buffer is a quite surprising observation. It suggests Trp residues are already mobility-restricted under these conditions. The pentamer is highly soluble and aggregation does not occur.

Therefore, the pentameric structure itself is responsible for the REES results. Quenching studies indicate that the STxB Trp residues remain at the membrane interface (5NS has a greater apparent quenching efficiency than 16NS and acrylamide is partially accessible to indoles). Carbohydrates are also able to quench Trp, at least to a physiologically relevant concentration (40–50 mM).

As a soluble globular protein, STxB runs at the membrane surface until it binds to its specific receptor Gb_3 [51]. STxB remains in a shallow position and pentameric even when interacting with the glycolipid. The overall results obtained in this study can be rationalised considering the model in Fig. 6. In the first stage, STxB binds five Gb_3 molecules in high affinity binding sites (site 2 in [28]), which are not in direct contact with Trp residues. Nevertheless, it induces micro-environment changes responsible for the increase in fluorescence intensity and lifetimes observed (up to 1.5 mM of vesicles). The protein might have the ability to cluster Gb_3 molecules in its vicinity, and site 1 and site 3 can bind the glycolipid upon saturation, as up to 15 Gb_3 analogues have been reported to attach to STxB. The third and less efficient binding site, which involves direct contact of the glycolipid with Trp residues, leads to the static quenching of fluorescence intensity observed at higher (above 1.5 mM) lipid concentration.

Acknowledgments

The authors would like to thank Prof. V.L. Shnyrov from Salamanca University (Spain) for fruitful discussions, and Dr. J. Ménétrey from Curie Institute (France), and S.T. Henriques from Lisbon University (Portugal) for valuable help. D.G. Pina was recipient of a postdoctoral fellowship from *Fundação para a Ciência e a Tecnologia*, Portugal (Ref. SFRH/BPD/14568/2003).

Appendix

Consider the partition/binding multi-equilibria depicted in:

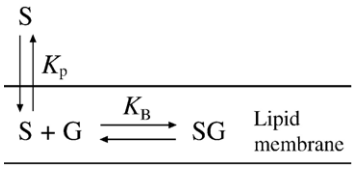

where S and G stand for the STxB monomer and Gb_3 respectively, and K_p and K_B are the equilibrium constants referring to membrane partition from buffer (W) to lipid (L) and binding in the lipid environment:

$$K_p = \frac{[S]_L}{[S]_W} \tag{A.1}$$

$$K_B = \frac{[SG]_L}{[S]_L[G]_L} \tag{A.2}$$

S is fluorescent due to the presence of a Trp residue. The fluorescence intensity, I, measured at given S, L, and G concentrations is:

$$I = I_{FW}X_{FW} + I_{FL}X_{FL} + I_{BL}X_{BL} \tag{A.3}$$

where I_{ij} refers to the limit fluorescence intensity that would be attained if all S molecules would be located in environment j (j=L, lipid; j=W, buffer) in conditions i (i=F, free, unbound; i=B, bound) and X_{ij} refers to the molar fraction of S meeting condition i and location j.

Assuming that the lipid concentration, [L], is such that the total lipid phase volume is much less than the aqueous phase volume and combining Eqs. (A.2) and (A.3):

$$\frac{I}{I_{SW}} = \left[[S]_W + b.\gamma_L[L].\frac{[G]_{T,L} - [G]_L}{K_B[G]_L} + c.\gamma_L[L]\left([G]_{T,L} - [G]_L\right)\right][S]_T^{-1} \tag{A.4}$$

$$b = \frac{I_{S,L}}{I_{S,W}} \tag{A.5}$$

$$c = \frac{I_{SG,L}}{I_{S,W}} \tag{A.6}$$

where γ_L is the molar volume of the lipid ($\gamma_L[L]$ is the volume fraction of the lipid) and $[G]_{T,L}$ is the total concentration of G in the lipid environment. $[S]_T$ is the total S concentration referring to the whole sample volume.

Combining Eqs. (A.1) and (A.2):

$$[G]_L = \frac{[G]_{T,L}}{K_pK_B[S]_W + 1} \tag{A.7}$$

$[S]_W$ is related to $[S]_T$ by:

$$[S]_W^2K_pK_B(1 + \gamma_L[L]K_p) + [S]_W[(1 + \gamma_L[L]K_p) + K_pK_B(\gamma_L[L][G]_{T,L} - [S]_T)] - [S]_T = 0 \tag{A.8}$$

that can be simplified to:

$$[S]_W^2.A + [S]_W.B + C = 0 \tag{A.9}$$

$$A = K_pK_B(1 + \gamma_L[L]K_p);$$
$$B = [(1 + \gamma_L[L]K_p) + K_pK_B(\gamma_L[L][G]_{T,L} - [S]_T)]; C = -[S]_T \tag{A.10}$$

and rearranged:

$$[S]_W = \frac{-B + \sqrt{B^2 - 4AC}}{2A} \tag{A.11}$$

Combining Eqs. (A.7) and (A..4):

$$\frac{I}{I_{SW}} = \left[(1 + b.\gamma_L[L]K_p) + c.\gamma_L[L][G]_{T,L}\frac{K_pK_B}{K_pK_B[S]_W + 1}\right]\frac{[S]_W}{[S]_T} \tag{A.12}$$

Eqs. (A.11) and (A.12) were used to fit the I/I_{SW} vs. [L] experimental data (keeping $[G]_{T,L}$ constant; Gb_3 5 mol%) and thus obtain c and K_B from non-linear regression (c=8.297±

2.404, $K_B = 0.0123 \pm 0.0051\ mM^{-1}$). K_p and b were previously obtained in a different experiment where pure lipid was used ($[G]_{T,L} = 0$). $K_p = 1400$ and $b = 0.113$ (see Fig. 5). It should be stressed that $K_B = 0.0123 \pm 0.0051\ mM^{-1}$ refers to the lipid phase volume, where the concentration of S and G are increased relative to the bulk analytical concentrations. This value can be converted to an apparent constant referring to bulk volume. Such apparent constant is much higher (by the order of the thousand, depending on [L]), however it does not describe the system adequately. It is the membrane partition and the binding effects combined that favor SG association, not only K_B by itself.

$c = 8.297 \pm 2.404$ reflects an apparently very high increase in quantum yield of SG relative to S in aqueous phase. This probably results from the extremely rigid lipid environment imposed by the Gb_3 ceramide tails to the indole residues of Trp34. Fig. 1 in the text show that these fluorophores in the pentamer structure may become caged in a ceramide ring.

References

[1] E.A. Merritt, W.G. Hol, AB_5 toxins, Curr. Opin. Struct. Biol. 5 (1995) 165–171.

[2] F. Proulx, E.G. Seidman, D. Karpman, Pathogenesis of Shiga toxin-associated hemolytic uremic syndrome, Pediatr. Res. 50 (2001) 163–171.

[3] P.O. Falnes, K. Sandvig, Penetration of protein toxins into cells, Curr. Opin. Cell Biol. 12 (2000) 407–413.

[4] K. Sandvig, B. van Deurs, Endocytosis, intracellular transport, and cytotoxic action of Shiga toxin and ricin, Physiol. Rev. 76 (1996) 949–966.

[5] L. Johannes, B. Goud, Surfing on a retrograde wave: how does Shiga toxin reach the endoplasmic reticulum? Trends Cell Biol. 8 (1998) 158–162.

[6] A.D. O'Brien, V.L. Tesh, A. Donohue-Rolfe, M.P. Jackson, S. Olsnes, K. Sandvig, A.A. Lindberg, G.T. Keusch, Shiga toxin: biochemistry, genetics, mode of action, and role in pathogenesis, Curr. Top. Microbiol. Immunol. 180 (1992) 65–94.

[7] K. Sandvig, O. Garred, K. Prydz, J.V. Kozlov, S.H. Hansen, B. van Deurs, Retrograde transport of endocytosed Shiga toxin to the endoplasmic reticulum, Nature 358 (1992) 510–512.

[8] F. Mallard, C. Antony, D. Tenza, J. Salamero, B. Goud, L. Johannes, Direct pathway from early/recycling endosomes to the Golgi apparatus revealed through the study of shiga toxin B-fragment transport, J. Cell Biol. 16 (1998) 973–990.

[9] T. Falguieres, F. Mallard, C. Baron, D. Hanau, C. Lingwood, B. Goud, J. Salamero, L. Johannes, Targeting of Shiga toxin B-subunit to retrograde transport route in association with detergent-resistant membranes, Mol. Biol. Cell 12 (2001) 2453–2468.

[10] A. Saint-Pol, B. Yélamos, M. Amessou, I.G. Mills, M. Dugast, D. Tenza, P. Schu, C. Antony, H.T. McMahon, C. Lamaze, L. Johannes, Clathrin adaptor epsinR is required for retrograde sorting on early endosomal membranes, Dev. Cell 6 (2004) 525–538.

[11] M. Amessou, V. Popoff, B. Yélamos, A. Saint-Pol, L. Johannes, Recent methods for studying retrograde transport, Curr. Prot. Cell Biol. (in press).

[12] C.A. Lingwood, Verotoxins and their glycolipid receptors, Adv. Lipid Res. 25 (1993) 189–211.

[13] J. Gariepy, The use of Shiga-like toxin 1 in cancer therapy, Crit. Rev. Oncol. Hematol. 39 (2001) 99–106.

[14] L. Johannes, D. Decaudin, Protein toxins: intracellular trafficking for targeted therapy, Gene Ther. 16 (2005) 1360–1368.

[15] K.-P. Janssen, D. Vignjevic, R. Boisgard, T. Falguières, G. Bousquet, D. Decaudin, F. Dollé, D. Louvard, B. Tavitian, S. Robine, L. Johannes, In vivo tumor targeting using a novel intestinal pathogen-based delivery approach, Cancer Res. 66 (2006) 7230–7236.

[16] O. Kovbasnjuk, R. Mourtazina, B. Baibakov, T. Wang, C. Elowsky, M.A. Choti, A. Kane, M. Donowitz, The glycosphingolipid globotriaosylceramide in the metastatic transformation of colon cancer, Proc. Natl. Acad. Sci. U. S. A. 102 (2006) 19087–19092.

[17] E.C. LaCasse, M.R. Bray, B. Patterson, W.M. Lim, S. Perampalam, L.G. Radvanyi, A. Keating, A.K. Stewart, R. Buckstein, J.S. Sandhu, N. Miller, D. Banerjee, D. Singh, A.R. Belch, L.M. Pilarski, J. Gariépy, Shiga-like toxin-1 receptor on human breast cancer, lymphoma, and myeloma and absence from $CD34^+$ hematopoietic stem cells: implications for ex vivo tumor purging and autologous stem cell transplantation, Blood 94 (1999) 2901–2910.

[18] H. Farkas-Himsley, R. Hill, B. Rosen, S. Arab, C.A. Lingwood, The bacterial colicin active against tumor cells in vitro and in vivo is verotoxin 1, Proc. Natl. Acad. Sci. U. S. A. 92 (1995) 6996–7000.

[19] D.C. Smith, J.M. Lord, L.M. Roberts, E. Tartour, L. Johannes, 1st class ticket to class I: protein toxin as pathfinders for antigen presentation, Traffic 3 (2002) 697–704.

[20] K. Sandvig, M. Ryd, O. Garred, E. Schweda, P.K. Holm, B. van Deurs, Retrograde transport from the Golgi complex to the ER of both Shiga toxin and the nontoxic Shiga B-fragment is regulated by butyric acid and cAMP, J. Cell Biol. 126 (1994) 53–64.

[21] L. Johannes, D. Tenza, C. Antony, B. Goud, Retrograde transport of KDEL-bearing B-fragment of Shiga toxin, J. Biol. Chem. 272 (1997) 19554–19561.

[22] M. Yu, D.B. Haslam, Shiga toxin is transported from the endoplasmic reticulum following interaction with the luminal chaperone HEDJ/ERdj3, Infect. Immun. 73 (2005) 2524–2532.

[23] J.M. Lord, L.M. Roberts, W.I. Lencer, Entry of protein toxins into mammalian cells by crossing the endoplasmic reticulum membrane: co-opting basic mechanisms of endoplasmic reticulum-associated degradation, Curr. Top. Microbiol. Immunol. 300 (2005) 149–168.

[24] N. Haicheur, E. Bismuth, S. Bosset, O. Adotevi, G. Warnier, V. Lacabanne, A. Regnault, C. Desaymard, S. Amigorena, P. Riccardi-Castagnoli, B. Goud, W.H. Fridman, L. Johannes, E. Tartour, The B subunit of Shiga toxin fused to a tumor antigen elicits CTL and targets dendritic cells to allow MHC class I-restricted presentation of peptides derived from exogenous antigens, J. Immunol. 165 (2000) 3301–3308.

[25] P.E. Stein, A. Boodhoo, G.J. Tyrell, J.L. Brunton, R.J. Read, Crystal structure of the cell-binding B oligomer of verotoxin-1 from *E. coli*, Nature 355 (1992) 748–750.

[26] M.E. Fraser, M.M. Chernaia, Y.V. Kozlov, N.G. James, Crystal structure of the holotoxin from *Shigella dysenteriae* at 2.5 A resolution, Nat. Struct. Biol. 1 (1994) 59–64.

[27] J.M. Richardson, P.D. Evans, S.W. Homans, A. Donohue-Rolfe, Solution structure of the carbohydrate-binding B-subunit homopentamer of verotoxin VT-1 from *E. coli*, Nat. Struct. Biol. 4 (1997) 190–193.

[28] H. Ling, A. Boodhoo, B. Hazes, M.D. Cummings, G.D. Armstrong, J.L. Brunton, R.J. Read, Structure of the shiga-like toxin I B-pentamer complexed with an analogue of its receptor Gb_3, Biochemistry 37 (1998) 1777–1788.

[29] H. Shimizu, R.A. Field, S.W. Homans, A. Donohue-Rolfe, Solution structure of the complex between the B-subunit homopentamer of verotoxin VT-1 from *Escherichia coli* and the trisaccharide moiety of globotriaosylceramide, Biochemistry 37 (1998) 11078–11082.

[30] A.M. Soltyk, C.R. MacKenzie, V.M. Wolski, T. Himara, P.I. Kitov, D.R. Bundle, J.L. Brunton, A mutational analysis of the globotriaosylceramide-binding sites of verotoxin VT1, J. Biol. Chem. 277 (2002) 5351–5359.

[31] W.K. Surewicz, K. Surewicz, H.H. Mantsch, F. Auclair, Interaction of Shigella toxin with globotriaosyl ceramide receptor-containing membranes: a fluorescence study, Biochem. Biophys. Res. Commun. 160 (1989) 126–132.

[32] D.G. Pina, J. Gómez, E. Villar, L. Johannes, V.L. Shnyrov, Thermodynamic analysis of the structural stability of the shiga toxin B-subunit, Biochemistry 42 (2003) 9498–9506.

[33] M.T. Saleh, J. Gariepy, Local conformational change in the B-subunit of Shiga-like toxin 1 at endosomal pH, Biochemistry 32 (1993) 918–922.

[34] L.D. Mayer, M.J. Hope, P.R. Cullis, Vesicles of variable sizes produced by a rapid extrusion procedure, Biochim. Biophys. Acta 858 (1986) 161–168.

[35] J.R. Lakowicz, Principles of Fluorescence Spectroscopy, 2nd ed.Plenum Press, New York, 1999.

[36] M.X. Fernandes, J.G. de La Torre, M.A.R.B. Castanho, Joint determination by Brownian dynamics and fluorescence quenching of the in-depth location profile of biomolecules in membranes, Anal. Biochem. 307 (2002) 1–12.
[37] M. Prieto, M.A.R.B. Castanho, A. Coutinho, F. Aranda, J.C.G. Fernandez, Fluorescence study of a derivatized diacylglycerol incorporated in model membranes, Chem. Phys. Lipids 69 (1994) 75–85.
[38] A.P. Demchenko, Red-edge-excitation fluorescence spectroscopy of single-tryptophan proteins, Eur. Biophys. J. 16 (1988) 121–129.
[39] A. Chattopadhyay, Exploring membrane organization and dynamics by the wavelength-selective fluorescence approach, Chem. Phys. Lipids 122 (2003) 3–17.
[40] D.G. Pina, J. Gómez, P. England, C.T. Craescu, L. Johannes, V.L. Shnyrov, Characterization of the non-native trifluoroethanol-induced intermediate conformational state of the Shiga toxin B-subunit, Biochimie 88 (2006) 1199–1207.
[41] A. Chattopadhyay, S.S. Rawat, D.A. Kelkar, S. Ray, A. Chakrabarti, Organization and dynamics of tryptophan residues in erythroid spectrin: Novel structural features of denatured spectrin revealed by the wavelength-selective fluorescence approach, Protein Sci. 12 (2003) 2389–2403.
[42] M.P. Brown, N. Shaikh, M. Brenowitz, L. Brand, The allosteric interaction between D-galactose and the *Escherichia coli* galactose repressor protein, J. Biol. Chem. 269 (1994) 12600–12605.
[43] W.D. Picking, J.A. McCann, A. Nutikka, C.A. Lingwood, Localization of the binding site for modified Gb_3 on verotoxin 1 using fluorescence analysis, Biochemistry 38 (1999) 7177–7184.
[44] S.W. Chui, E. Jakobsson, S. Subramainian, H.L. Scott, Combined Monte Carlo and molecular dynamics simulation of fully hydrated dioleyl and palmitoyl-oleyl phosphatidylcholine lipid bilayers, Biophys. J. 77 (1999) 2462–2469.
[45] N.C. Santos, M. Prieto, M.A.R.B. Castanho, Interaction of the major epitope region of HIV gp41 with membrane model systems. A fluorescence spectroscopy study, Biochemistry 37 (1998) 8674–8682.
[46] N.C. Santos, M. Prieto, M.A.R.B. Castanho, Quantifying molecular partition into model systems of biomembranes: an emphasis on optical spectroscopic methods, Biochim. Biophys. Acta 1612 (2003) 123–135.
[47] D.G. Pina, L. Johannes, Cholera and Shiga toxin B-subunits: thermodynamic and structural considerations for function and biomedical applications, Toxicon 45 (2005) 389–393.
[48] Y.U. Katagiri, T. Mori, H. Nakajima, C. Katagiri, T. Taguchi, T. Takeda, N. Kiyokawa, J. Fujimoto, Activation of src family kinase yes induced by shiga toxin binding to globotriaosyl ceramide (Gb3/CD77) in low density, detergent-insoluble microdomains, J. Biol. Chem. 274 (1999) 35278–35282.
[49] O. Kovbasnjuk, M. Edidin, M. Donowitz, Role of lipid rafts in Shiga toxin 1 interaction with the apical surface of Caco-2 cells, J. Cell Sci. 114 (2001) 4025–4031.
[50] P. Sharma, R. Varma, R.C. Sarasij, Ira, K. Gousset, G. Krishnamoorthy, M. Rao, S. Mayor, Nanoscale organization of multiple GPI-anchored proteins in living cell membranes, Cell 116 (2004) 577–589.
[51] M.A.R.B. Castanho, M.X. Fernandes, Lipid membrane-induced optimization for ligand-receptor docking: recent tools and insights for the "membrane catalysis" model, Eur. Biophys. J. 35 (2006) 92–103.